Additive manufacturing of a novel in-situ alloyed AISI316L-Cu stainless steel: Microstructure and antibacterial properties

Additive manufacturing of a novel in-situ alloyed AISI316L-Cu stainless steel: Microstructure and Antibacterial properties

Amir Behjat[a,b], Morteza Shamanian[b], Fazollolah Sadeghi[c], Luca Iuliano[a], Abdollah Saboori[a,*]

[a] *Integrated Additive Manufacturing Center, Department Management and Production Engineering, Politecnico di Torino, Corso Duca Degli Abruzzi 24,10129 Torino, Italy*

[b] *Department of Materials Engineering, Isfahan University of Technology, 84156-83111 Isfahan, Iran*

[c] *Graduate Institute of Ferrous and Energy Materials Technology, Pohang University of Science and Technology, Pohang, 37673, Republic of Korea*

**Corresponding author: Abdollah.saboori@polito.it, +39-0110907285*

Abstract

Developing antibacterial metal implants is an innovative approach to reducing the risk of implant-related infections. In order to clarify the in-situ effect of copper contents on the microstructure and antibacterial properties of AISI316L stainless steel for advanced applications, Cu-bearing stainless steel was developed by the mean of the laser powder bed fusion process. This work demonstrates that using in-situ alloying with Cu addition can significantly promote antimicrobial activity against Escherichia coli and Staphylococcus aureus without significantly affecting microstructures. This methodology would apply to developing novel metallic materials towards new engineering applications of multi-function.

Keywords: Laser powder bed fusion, AISI316L stainless steel, In-situ alloying, Antimicrobial activity.

1. Introduction

Metallic materials are commonly employed in producing various implantable devices, including those intended for orthopedic, vascular, and other purposes [1]. Among them, AISI316L stainless steel has emerged as a popular choice mainly owing to its favorable mechanical properties, corrosion resistance, and cost-effectiveness. Currently, the use of this alloy for the production of implants is commonly associated with severe and devastating bacterial infections. Such infections often lead to significant pain and financial burdens for patients [2,3]

Over the past years, there has been an emergence of new medical metallic materials with antibacterial properties. It is well documented that the effectiveness of antibacterial metallic implants depends highly on the design of the implant material [4]. Therefore, appropriate selection and integration of antibacterial agents into the implant material are crucial to ensure constant effective antibacterial activity throughout the lifespan of the implants. It is well reported a wide range of antibacterial agents include metallic ions like Cu, Ag, and Zn can be used in the production of antibacterial metallic implants [5,6]. The selection of a particular antibacterial agent depends on several factors, including effectiveness, safety, compatibility with the implant material and cost [7]. Among them, Cu, a trace element in the human body, does not interfere with normal metabolic processes. Additionally, Cu is widely employed as an alloying element in orthopedic implants due to its proven effectiveness in preventing bacterial growth and promoting bone formation [8,9]

Additive Manufacturing (AM) technology for metallic components is a modern process that offers design flexibility and fast production time [10,11]. Nevertheless, the number of materials that can be processed via these technologies and fulfil all biomedical application criteria is limited. Hence material development for AM technologies could attract lots of attention [12]. One of the main advantages of using AM for alloy development is the ability to precisely control the composition and microstructure of material [13].In particular, in-situ alloying of elemental powders using powder fusion-based AM could gain popularity due to its efficiency and cost-effectiveness in developing new alloys. Up to now, The addition of elements into AISI316L fabricated with AM has been the focus of numerous studies, including Ti [14], Ag [15], and CrN [16]. Despite all the efforts, far too little attention has been paid to the development of antibacterial AISI316 alloys by AM [3].Therefore, this study aims to examine the effect of Cu addition on the microstructural and antimicrobial characteristics of AISI316L fabricated by L-PBF process.

2. Materials and methods

To produce the initial feedstock material, a gas atomized spherical AISI316L powder (Oerlikon, 15-45 μm) and pure elemental Cu powder (Sandvik Osprey Ltd., 3-5 μm) were mixed in a jar mill for 16 hrs. The resulting composition of the AISI316L-Cu was Fe-17Cr-12Ni-2Mo-3.5Cu in weight percentage. An M-Lab CusingR Concept Laser machine equipped with a 100 W fiber laser under an argon gas environment was employed to print samples. Specific processing parameters included the laser power of 95 W, the scan speed of 500 mm/s and hatch spacing of 84 μm. Each layer was scanned in a zigzag pattern, rotated by 67 degrees between each successive layer. In order to serve as a control group, AISI316L samples were also fabricated using the same method. A Scanning Electron Microscope (SEM) equipped with Electron Back Scattered Diffraction (EBSD) technique was utilized to analyze the microstructures. The antibacterial performance was assessed using the plate count method against *Escherichia coli* ATCC25922 (*E. coli*) and *Staphylococcus aureus* ATCC25923 (*S. aureus*) bacteria. The samples were soaked in bacteria suspension (10^5 CFU mL^{-1}) at 37 °C for 24 h. The details of this method were reported in previous works [6,7]. The number of bacteria was counted to evaluate the antibacterial properties of the samples. The equation used to determine the antibacterial rate *C* is as follows:

$$C\ (\%) = (A - B)/A \times 100 \tag{1}$$

Here, A and B represents the number of bacterial colonies present in the AISI316L and AISI316L-Cu alloy, respectively..

3. Results and discussion

Fig. 1 (a,b) shows the cross-section of samples characterized by grains with irregular shapes and wavelike grain boundaries, in which it could be attributed to the temperature gradient generated through laser scanning and the rapid solidification during the L-PBF process. The EDS map of Cu is displayed in Fig. 1(c). It suggests that the Cu powders were fully dissolved into the austenitic phase during printing, with no notable segregation of Cu content. This finding is in line with the X-ray diffraction patterns shown in Fig. 1 (d), which indicate that the AISI316L-Cu sample only contains the austenite phase, without any additional peaks corresponding to ε-Cu phases. According to the Bragg equation, the decrease of the peak angle corresponding to the austenite phase indicated the increase of lattice distance (Fig. 1(e)). This result indicating that the solid solution of Cu causes slight increase in a lattice distortion of austenite phase. In addition, changing cooling rate by adding Cu to the AISI316L feedstock causes decreasing crystallite size of AISI316L sample. Overall, in-situ alloying AISI316L by Cu using L-PBF caused finer crystallite size and higher microstrain, resulting higher hardness value and slight better mechanical properties (Fig 1(e)).

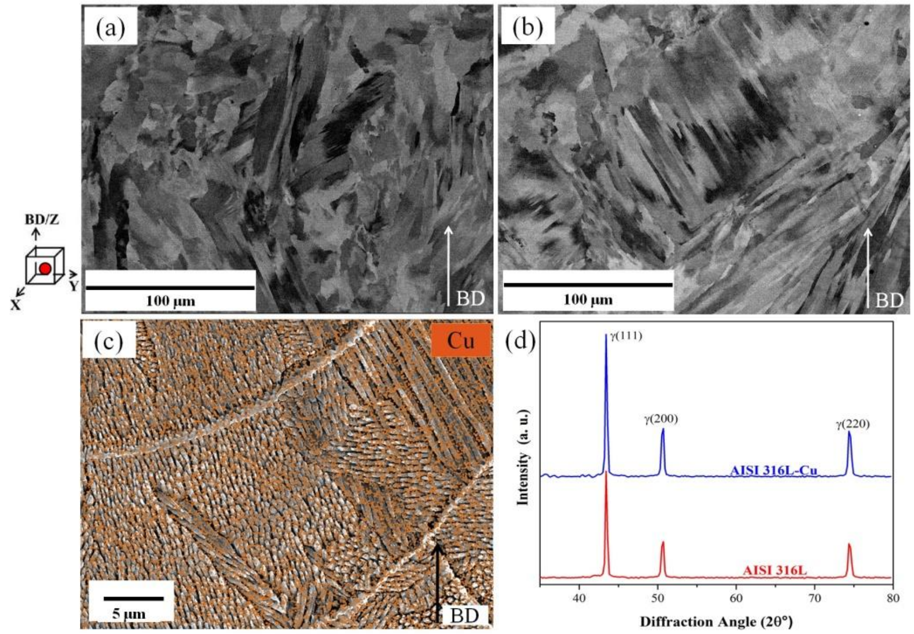

(e)

Sample	2 θ (°)	FWHM (rad)	Crystallite size (A°)	Micro strain (%)	Hardness (HV)	YS (MPa)	UTS (MPa)	Elongation (%)
LPBFed AISI316L	43.624	0.385	221	4.23	228±7	500±8	536±11	28.6±1.1
LPBFed AISI316L-Cu	43.452	0.475	147	6.37	245±8	510±7	558±6	30.4±1.4

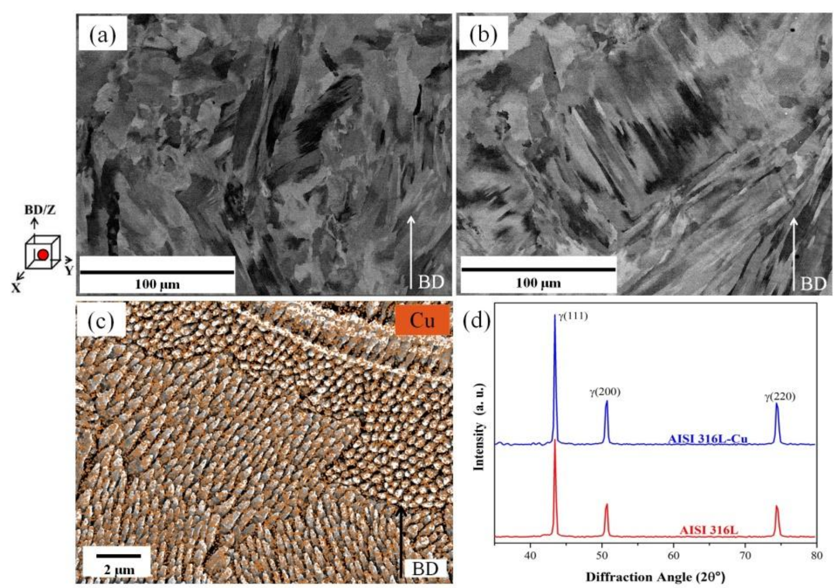

(e)

Sample	2 θ (°)	FWHM (rad)	Crystallite size (A°)	Micro strain (%)	Hardness (HV)	YS (MPa)	UTS (MPa)	Elongation (%)
LPBFed AISI316L	43.624	0.385	221	4.23	228±7	500±8	536±11	28.6±1.1
LPBFed AISI316L-Cu	43.452	0.475	147	6.37	245±8	510±7	558±6	30.4±1.4

Fig. 1. SEM micrograph from the cross-section of the (a), AISI316L, (b) AISI316L-Cu, (c) EDS Cu element measurements, (d) XRD analysis, and (e) mechanical properties and data obtained from XRD pattern.

Fig. 2 presents the morphology characterization of as-built samples through the EBSD analysis. As shown in Fig. 2(a,d),The image quality with grain boundaries distributions of samples indicates that the AISI316-Cu alloy had a slight fine grain size as compared with the AISI316L sample. Fig. 2 (g,h) shows the grain size and percentages of low and high angle grain boundaries. The addition of Cu into the alloy resulted in a higher rate of heat transfer within the molten pool, in which provided a stronger driving force for the solidification process, resulting in grain refinement. Indeed, it is well known that existence of higher low angle grain boundaries for the AISI316L-Cu sample can be attributed to the rapid cooling of molten material. Fig. 2(b,e)displays the inverse pole figures (IPF-Z), where the grains of the both samples had similar shapes. In addition, our results show that the Cu had little influence on the texture development and there is no evident texturing for both samples. This is attributed to the rotation strategy scanning applied during the L-PBF process. The distributions of Kernel Average Misorientation (KAM) are displayed in Fig. 2(c,f). As illustrated, the KAM value at the grain boundaries is higher than within the grains. This difference indicates a greater dislocation density formed around the grain boundaries in both alloys.

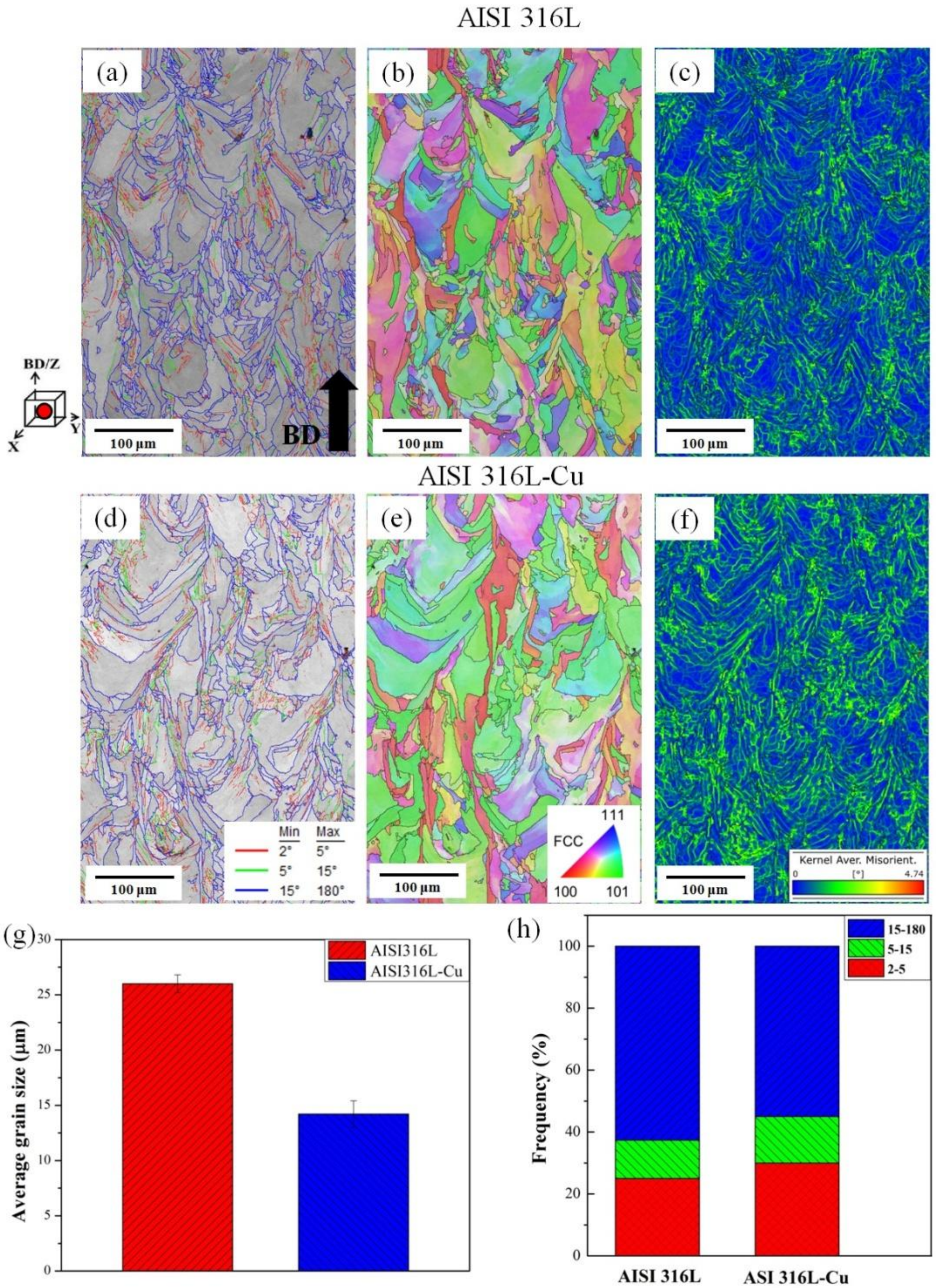

Fig. 2. Results of EBSD analysis for the as-built (a–c) AISI316L, (d-f) AISI316L-Cu samples, (g) average grain size, and (h) fraction of low and high angle grain boundaries.

Fig. 3(a) presents the antibacterial rate of the AISI316L-Cu alloy against *S. aureus* and *E. coli* bacterial, and the corresponding representative bacterial colony images shown in Fig. 3(b). The results indicate that after 24 hours of incubation, the petri-dish of AISI316L was entirely covered with bacterial colonies. Conversely, only a few bacterial colonies were found for AISI316L-Cu, demonstrating that copper addition successfully eradicated nearly all the bacteria and improved the material's antibacterial characteristics. According to Eq.1, the antibacterial rates of AISI316L-Cu against *S. aureus* and *E. coli* were 93.4 ± 1.2% and 97.8 ± 0.8%, respectively. According to previous reports, variation in the antibacterial efficacy against bacteria might be attributed to the disparity in the thickness of the cell wall between *E.coli* (7-8 nm) and *S.aureus* (20-80 nm) [6]. Consequently, it can be reasonably deduced that the AISI316L-Cu alloy exhibited strong antibacterial ability against *E.coli* and *S. aureus* being relatively hard to be killed.

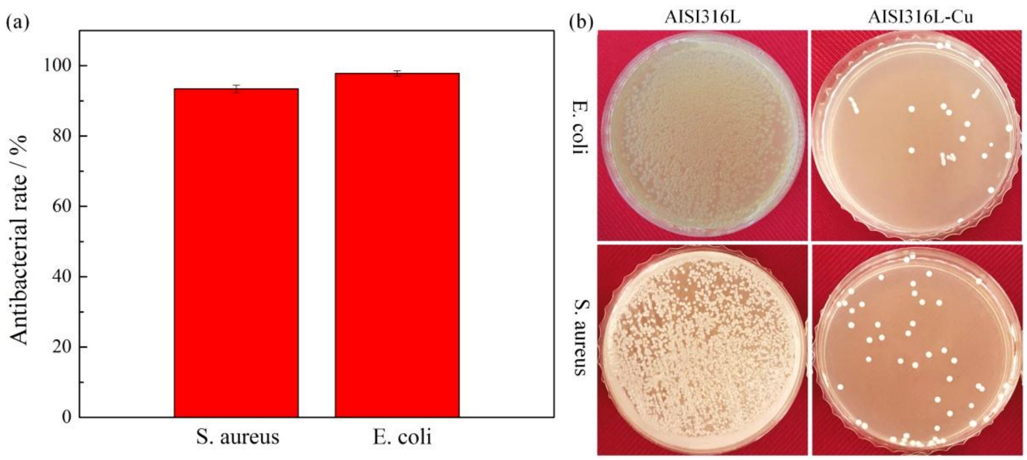

Fig. 3. (a) Antibacterial rate of AISI316L-Cu with S. aureus and E. coli, (b) corresponding bacterial colonies in petri dishes.

The morphology of bacterial biofilms on the surfaces of the experimental materials was carried out using SEM. As presented in Fig. 4, ball-shaped *S. aureus* and strip-shaped *E. coli* were found to have formed noticeable biofilms on the AISI316L surfaces. In these biofilms, numerous bacteria were observed to be stacked and intertwined, creating multilayer structures. Although a few randomly dispersed bacteria were present on the surface of AISI316L-Cu, no distinct bacterial biofilms were detected. This implies that the surface of AISI316L-Cu is not easily susceptible to bacterial adhesion and, thus, can effectively prevent the formation of bacterial biofilms on its surface.

The mechanism behind the antibacterial properties of AISI316L-Cu can be attributed to the release of copper ions from the surface when it comes into contact with aqueous media [4]. Indeed, it is stated that changes in the valence state of Cu ions are responsible for adsorbing electrons from bacteria upon their release from the surface [7]. Additionally, the formation of a thin layer of copper oxide on the surface of AISI316L-Cu material can also serve as an effective antibacterial mechanism [8]. . These mechanisms, in combination, work towards reducing the likelihood of implant-associated infections, which has been confirmed by the AISI316L-Cu studied in this work.

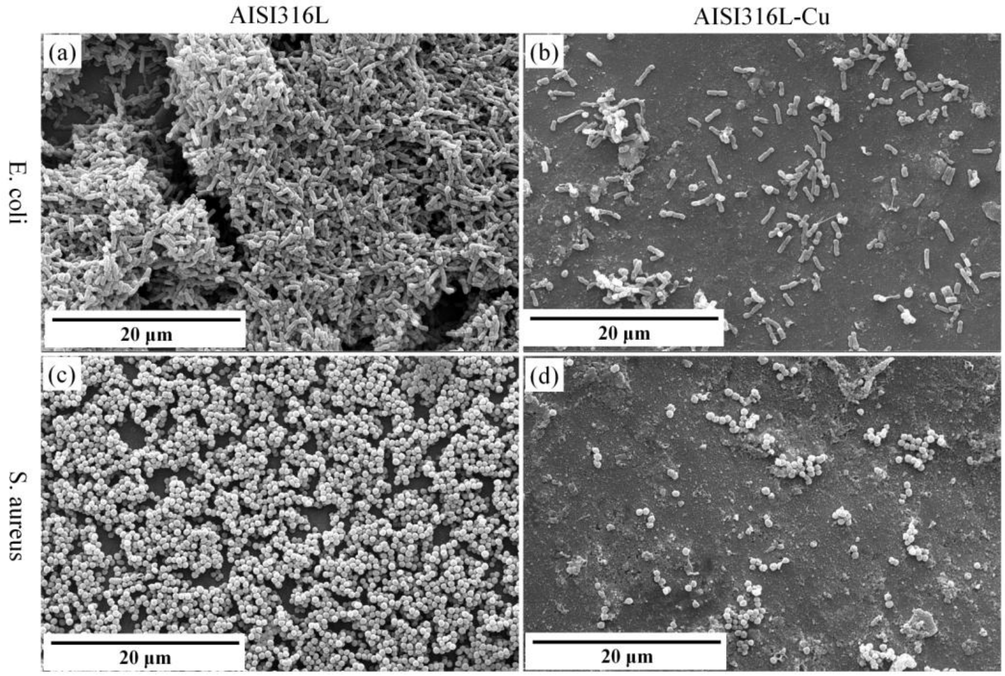

Fig. 4. SEM images of E. coli (a,b), and S. aureus (c,d) on surfaces of AM AISI316L and AISI316L-Cu.

4. Conclusions

In the present work, a novel material for the L-PBF process was designed and produced following the in-situ alloying approach. The findings confirm that integrating copper into stainless steel by AM has the potential to offer a novel approach to curbing the spread of bacterial infections in a variety of contexts, including hospitals, food production facilities, medical implants and public areas. All in all, it can be concluded that material development for AM through the in-situ alloying approach presents new opportunities for producing cost-effective and efficient materials with tailored properties for specific applications.

References

[1] N.S. Manam, W.S.W. Harun, J. Alloys Compd. 701 (2017) 698–715.

[2] D. Campoccia, L. Montanaro, Biomaterials. 34 (2013) 8018–8029.

[3] Q. Wang, L. Ren, X. Li, Mater. Sci. Eng. C. 68 (2016) 519–522.

[4] J. Jiao, S. Zhang, Front. Cell. Infect. Microbiol. 11 (2021).

[5] C.A. Biffi, J. Fiocchi, Mater. Lett. 335 (2023) 133749.

[6] L. Ren, K. Yang, Mater. Sci. Eng. C. 32 (2012) 1204–1209.

[7] E. Zhang, X. Zhao, J. Hu, Bioact. Mater. 6 (2021) 2569–2612.

[8] E.-L. Zhang, S. Fu, Rare Met. 38 (2019) 476–494.

[9] Z. Yuan, T. Xi, Mater. Lett. 272 (2020) 127815.

[10] A. Behjat, M. Shamanian, A. Saboori, L. Iuliano, J. Mater. Res. Technol. 23 (2023) 3294–3311.

[11] E. Davoodi, H. Montazerian, Bioact. Mater. 15 (2022) 214–249.

[12] M.H. Mosallanejad, B. Niroumand, J. Alloys Compd. 857 (2021)

[13] M.H. Mosallanejad, A. Saboori, J. Alloys Compd. 872 (2021) 159567.

[14] W. Zhai, W. Zhou, Mater. Sci. Eng. A. 840 (2022) 142912.

[15] J. Quan, K. Lin, D. Gu, Powder Technol. 364 (2020) 478–483.

[16] V.B. Vukkum, J. Christudasjustus, Npj Mater. Degrad. 6 (2022) 1–11.